Crystal Structure and Single Crystal ^{35}Cl NQR of 1,2-Dichloro-3-Nitrobenzene, $Cl^{(1)}Cl^{(2)}(NO_2)^{(3)}C_6H_3$ *

Surendra Sharma, Helmut Paulus, Norbert Weiden, and Alarich Weiss
Institut für Physikalische Chemie, Physikalische Chemie III, Technische Hochschule Darmstadt

Z. Naturforsch. **41 a,** 134–140 (1986); received August 2, 1985

1,2-Dichloro-3-nitrobenzene, $Cl^{(1)}Cl^{(2)}(NO_2)^{(3)}C_6H_3$, was investigated by X-ray diffraction and single crystal ^{35}Cl NQR Zeeman spectroscopy. The crystal structure was determined, $R_w = 0.033$. The compound crystallizes with the space group $C_{2h}^5 - P2_1/c$, $Z = 4$; $a = 381.0(1)$ pm, $b = 1376.5(3)$ pm, $c = 1430.2(3)$ pm, $\beta = 97.764(5)°$. From the ^{35}Cl NQR Zeeman spectra it was found at 294 K: $e^2\Phi_{zz}Qh^{-1}(^{35}Cl^{(1)}) = 71.892(6)$ MHz, $\eta(^{35}Cl^{(1)}) = 0.1287(25)$, $e^2\Phi_{zz}Qh^{-1}(^{35}Cl^{(2)}) = 75.436(6)$ MHz, $\eta(^{35}Cl^{(2)}) = 0.1525(25)$. The angles ($\Phi_{zz}^{(1)}$, $\Phi_{zz}^{(2)}$) and ($\Phi_{zz}^{(2)}$, $C^{(3)}-N^{(3)}$) are slightly opened in comparison to the corresponding X-ray bond angles. The temperature dependence of $\nu(^{35}Cl)$ is reported.

Introduction

In the course of our studies on the magnitude and orientation of electric field gradient tensors, EFGT, in benzene derivatives [1–3] we have chosen 1,2-dichloro-3-nitrobenzene, $Cl^{(1)}Cl^{(2)}(NO_2)^{(3)}C_6H_3$ as one of the compounds of interest. It crystallizes well from alcoholic solution in the form of prisms. The light yellow solid was investigated by Jaeger [4] crystallographically and described as orthorhombic bipyramidal. Later it was found that 1,2-dichloro-3-nitrobenzene crystallizes in the monoclinic system [5]. The pyknometric density of the compound is 1.721 Mgm^{-3} [4]. The question arises as to how three rather strongly electronegative substituents (two chlorines and one NO_2 group) influence the asymmetry parameter η and the orientation of the EFGT at the ^{35}Cl sites.

Experimental

Large single crystals were grown from the melt for the ^{35}Cl NQR spectroscopy by the Bridgeman technique. The growth direction was [100]. The crystal structure was determined at 293 K using small samples. Appropriate absorption corrections were applied. The relevant data of the structure determination are given in Table 1.

The single crystal Zeeman split NQR measurements were done at 294 K on the 4π-Zeeman goniometer described earlier [6]. Fourier transform technique was applied for the single crystal sudies as well as for the measurements of $\nu(^{35}Cl) = f(T)$ on powder samples. The orientation of the crystal used for the Zeeman spectroscopy was checked by X-ray diffraction. Its orientation with respect to the Zeeman coil system is shown in Figure 1. The measurements of $\nu(^{35}Cl) = f(T)$ were done by maintaining the desired temperature at the sample by a flow of temperature regulated gaseous nitrogen.

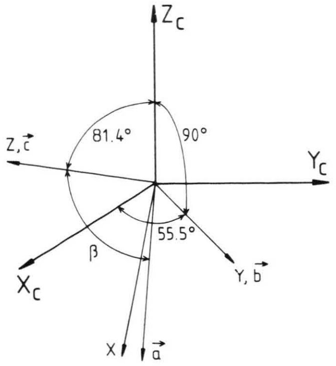

Fig. 1. Coordinate system used throughout the paper. X_c, Y_c, Z_c is the laboratory system which coincides with the axes of the three mutually perpendicular Helmholtz coils of the 4π Zeeman goniometer. The axis $\boldsymbol{a}$ of the crystal coincides with Z_c. The orthogonal axes system X, Y, Z is chosen in such a way that $\boldsymbol{b} \parallel Y$, $\boldsymbol{c} \parallel Z$, from which choice $\sphericalangle (X, \boldsymbol{a}) = \beta - 90° = 7.76°$ follows.

---

* Presented at the VIIIth International Symposium on Nuclear Quadrupole Resonance Spectroscopy, Darmstadt, July 22–26, 1985.

Reprint requests to Prof. A. Weiss, Institut für Physikalische Chemie, Physikalische Chemie III, Technische Hochschule Darmstadt, Petersenstraße 20, D-6100 Darmstadt, West-Germany.

0340-4811 / 86 / 0100-0134 $ 01.30/0. – Please order a reprint rather than making your own copy.

Table 1. Experimental conditions and crystal data of 1,2-dichloro-3-nitrobenzene, $Cl^{(1)}Cl^{(2)}(NO_2)^{(3)}C_6H_3$.

Experimental conditions		Crystal data	
Habitus, size	needle ∥ [001] 0.2 × 0.2 × 0.8 mm	Lattice constants	
Diffractometer	Stoe-Siemens AED2	a/pm	381.0(1)
Wavelength, λ/pm	71.073 (Mo Kα)	b/pm	1376.5(3)
Temperature, K	293	c/pm	1430.2(3)
Linear absorption coefficient, μ/m^{-1}	737	β/degree	97.764(5)
Scan	ϑ/ω	Space group	$C_{2h}^5-P2_1/c$
$(\sin\vartheta/\lambda)_{max}$, pm^{-1}	0.0070	formula units/ unit cell	4
Measured reflections	3553		
Symmetry independent reflections	1649	ϱ_{calc}/Mgm^{-3}	1.716
Reflection considered	1549		
$R(F)$	0.036		
$R_w(F)$	0.033		

Numbering of the atoms in the molecule

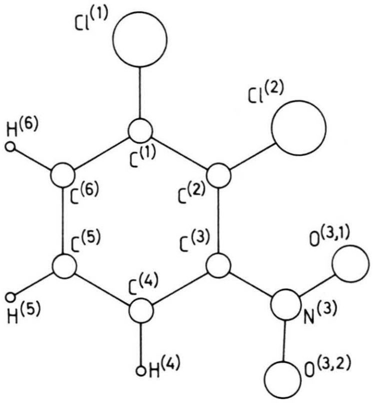

Point positions:

All atoms in 4(e):

$x, y, z;\quad \bar{x}, \bar{y}, \bar{z};\quad \bar{x}, \frac{1}{2}+y, \frac{1}{2}-z;\quad x, \frac{1}{2}-y, \frac{1}{2}+z$

Table 2. Positional and thermal parameters (with standard deviations) of 1,2-dichloro-3-nitrobenzene. X-ray diffraction results. The temperature factor is of the form

$$T = \exp\{-2\pi^2(U_{11}h^2a^{*2} + U_{22}k^2b^{*2} + U_{33}l^2c^{*2} + 2U_{12}hka^*b^* + 2U_{13}hla^*c^* + 2U_{23}klb^*c^*)\}.$$

The U_{ij} are given in (pm)^2. U is the isotropic mean square thermal amplitude. The occupancy factor is 1.0 for each atom.

Atom	x/a	y/b	z/c	U_{11} or U	U_{22}	U_{33}	U_{12}	U_{13}	U_{23}
Cl$^{(1)}$	0.15893(15)	−0.03830(3)	0.37368(4)	668(4)	577(3)	686(3)	193(2)	119(3)	19(2)
Cl$^{(2)}$	−0.00069(14)	−0.01478(3)	0.15405(3)	606(3)	489(2)	662(3)	−72(2)	−34(2)	−133(2)
O$^{(3,1)}$	0.01012(57)	0.25503(12)	0.05668(10)	1235(15)	823(10)	615(9)	294(11)	−81(10)	162(7)
O$^{(3,2)}$	0.30835(53)	0.12885(11)	0.03020(9)	1271(16)	902(11)	501(8)	151(11)	203(9)	−71(8)
N$^{(3)}$	0.18569(48)	0.18441(11)	0.08255(11)	681(11)	559(9)	436(8)	−26(8)	20(8)	14(7)
C$^{(1)}$	0.26030(46)	0.06919(12)	0.32051(11)	397(9)	454(8)	472(9)	53(7)	71(8)	47(7)
C$^{(2)}$	0.18652(43)	0.07867(11)	0.22308(11)	339(9)	401(8)	474(9)	25(7)	22(7)	−54(6)
C$^{(3)}$	0.26030(46)	0.16793(11)	0.18492(11)	405(9)	460(8)	393(8)	30(7)	42(7)	−6(7)
C$^{(4)}$	0.40105(52)	0.24445(13)	0.23963(13)	506(11)	429(9)	560(11)	−26(8)	63(9)	−4(7)
C$^{(5)}$	0.47893(57)	0.23147(13)	0.33528(13)	567(12)	507(10)	538(11)	−21(9)	−18(9)	−154(8)
C$^{(6)}$	0.40800(54)	0.14433(13)	0.37573(13)	565(12)	595(11)	398(9)	66(9)	25(8)	−35(8)
H$^{(4)}$	0.45831(526)	0.30058(135)	0.21200(126)	600					
H$^{(5)}$	0.57272(541)	0.27935(130)	0.37146(126)	600					
H$^{(6)}$	0.45936(538)	0.13548(122)	0.44201(128)	600					

The temperature was measured with a thermocouple to an accuracy of ± 0.3 K.

Results

In Table 1 the crystallographic data of $Cl^{(1)}Cl^{(2)}(NO_2)^{(3)}C_6H_3$ are given together with some experimental data. The results of the crystal structure determination are shown in Tables 2–5. Table 2 gives the positional and thermal parameters. In Table 3 the intermolecular distances are listed. Table 4 contains the coordinates of the "best plane" through the benzene ring and the distances of the atoms of the molecule from this plane.

^{35}Cl NQR measurements on the polycrystalline $Cl^{(1)}Cl^{(2)}(NO_2)^{(3)}C_6H_3$ have been reported at room temperature [7, 8] and at 297 and 90 K [9]. The temperature dependence over the entire range from 77 K to the melting point (334 K) is shown in Figure 2. There is no evidence of a phase transition in that range. Rationalisation of the curve $\nu(^{35}Cl) = f(T)$ according to $\nu(^{35}Cl) = \sum_i a_i T^i$ yields the values given in Table 5.

Table 3. Intermolecular distances (selected values) of 1,2-dichloro-3-nitrobenzene, $Cl^{(1)}Cl^{(2)}(NO_2)^{(3)}C_6H_3$.

Atoms	Distance [pm]	Atoms	Distance [pm]
$Cl^{(1)} \ldots O^{(3,1)}$	311.0	$Cl^{(2)} \ldots H^{(5)}$	331.4
$Cl^{(1)} \ldots H^{(4)}$	300.5	$O^{(3,1)} \ldots H^{(5)}$	297.1
$Cl^{(1)} \ldots H^{(6)}$	313.3	$O^{(3,1)} \ldots H^{(6)}$	294.1
$Cl^{(1)} \ldots Cl^{(1)}$	410.1	$O^{(3,2)} \ldots H^{(5)}$	289.5
$Cl^{(2)} \ldots O^{(3,2)}$	315.4		

Table 4. Intramolecular "best" ring plane and deviations d from this plane. The cartesian system used is $y \parallel \boldsymbol{b}$, $z \parallel \boldsymbol{c}$, and $\sphericalangle(\boldsymbol{a}, x) = \beta - 90°$.

$$-0.9182x + 0.3208y + 0.2325z - 0.4270 = 0$$

Atom	d/pm	Atom	d/pm
$C^{(1)}$	− 1.1	$Cl^{(1)}$	− 7.6
$C^{(2)}$	0.7	$Cl^{(2)}$	− 2.2
$C^{(3)}$	0.4	$N^{(3)}$	0.4
$C^{(4)}$	− 1.1	$O^{3,1)}$	− 85.1
$C^{(5)}$	0.8	$O^{(3,2)}$	86.3
$C^{(6)}$	0.4		

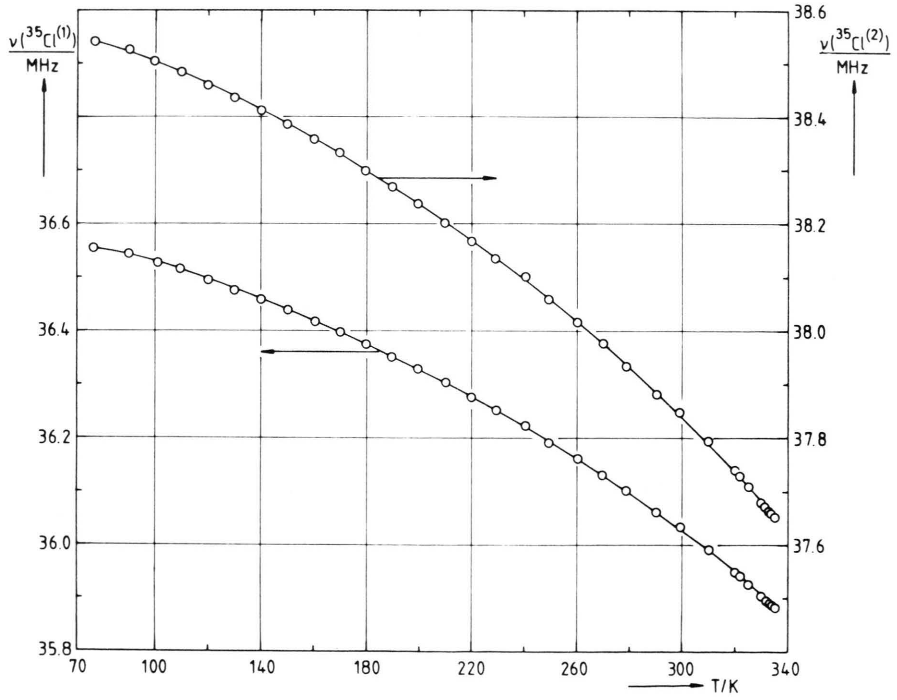

Fig. 2. ^{35}Cl NQR frequencies of $Cl^{(1)}Cl^{(2)}(NO_2)^{(3)}C_6H_3$ as a function of temperature.

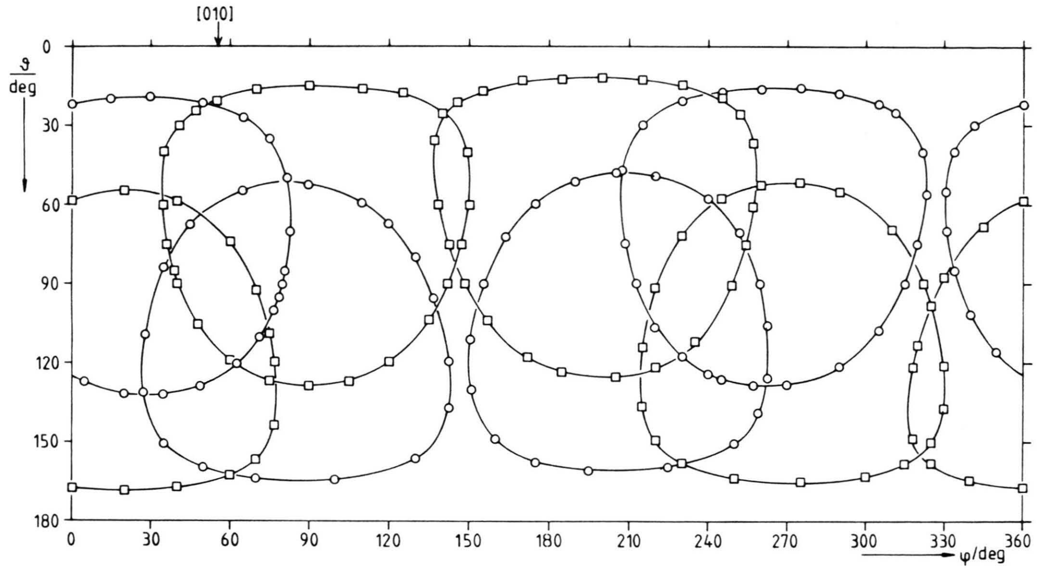

Fig. 3. Zero splitting cones ϑ_0, φ_0 of ^{35}Cl NQR in $Cl^{(1)}Cl^{(2)}(NO_2)^{(3)}C_6H_3$. The angles ϑ and φ are given with respect to the laboratory system X_c, Y_c, Z_c, see Figure 1. ○ $Cl^{(1)}$; □ $Cl^{(2)}$. $T = 294$ K.

Table 5. Parametrization of $\nu(^{35}Cl) = f(T)$ for the range $77 \leqq T/K \leqq 334$. $\nu(^{35}Cl) = \sum_i a_i T^i$.

Atom	a_{-1} [MHz K]	a_0 [MHz]	$a_1 \cdot 10^4$ [MHz K^{-1}]	$a_2 \cdot 10^6$ [MHz K^{-2}]
$Cl^{(1)}$	5.626	36.5022	3.128	− 6.571
$Cl^{(2)}$	6.438	38.5051	1.797	− 8.241

Table 6. ^{35}Cl frequency, nuclear quadrupole coupling constant $e^2 \Phi_{zz} Q h^{-1}(^{35}Cl)$, and asymmetry parameter $\eta(^{35}Cl)$.

Atom	$\nu(^{35}Cl)$ $T = 77$ K [MHz]	$\nu(^{35}Cl)$ $T = 294$ K [MHz]	$e^2 \Phi_{zz} Q h^{-1}(^{35}Cl)$ $T = 294$ K [MHz]	$\eta(^{35}Cl)$ $T = 294$ K
$Cl^{(1)}$	36.556(3)	36.045(3)	71.892(6)	0.1287(25)
$Cl^{(2)}$	38.543(3)	37.864(3)	75.436(6)	0.1525(25)

Table 7. Direction cosines of the principal axes Φ_{xx}, Φ_{yy}, and Φ_{zz} of the EFGTs and of the bond directions $C^{(j)}-Cl^{(j)}$; $j = 1, 2$, with the orthogonal axes system X, Y, Z (see Fig. 1) in 1,2-dichloro-3-nitrobenzene at $Z = 294$ K.

Atom	Φ_{vv}	$\lambda^{(j)}$	$\mu^{(j)}$	$\nu^{(j)}$
$Cl^{(1)}$	Φ_{xx}	0.91182	− 0.35022	− 0.21414
	Φ_{yy}	0.35320	0.40321	0.84429
	Φ_{zz}	− 0.20947	− 0.84542	0.49131
$Cl^{(2)}$	Φ_{xx}	0.90695	− 0.38592	− 0.16836
	Φ_{yy}	− 0.06813	− 0.52949	0.84553
	Φ_{zz}	− 0.41547	− 0.75529	− 0.50665
Bond	$C^{(j)}-Cl^{(j)}$			
	$C^{(1)}-Cl^{(1)}$	− 0.22109	− 0.85482	0.46947
	$C^{(2)}-Cl^{(2)}$	− 0.41163	− 0.74921	− 0.51890

Figure 3 shows the zero splitting positions ϑ_0, φ_0 for the two chemically (and therefore also crystallographically) inequivalent Cl-atoms. Due to the 4π geometry of the Zeeman goniometer all zero-splitting cones for the 4 atoms of $Cl^{(1)}$ as well as the 4 atoms of $Cl^{(2)}$ of the unit cell ($Z = 4$, see Table 1) are experimentally located. The cones connected by the operation i are of course indistinguishable from each other. By the usual procedure from the zero-splitting cones and the resonance frequencies in zero field the nuclear quadrupole coupling constants $e^2 \Phi_{zz} Q h^{-1}$ and the asymmetry parameters η are found from the relations

$$\nu(^{35}Cl) = \frac{1}{2} e^2 \Phi_{zz} Q h^{-1} \left(1 + \frac{\eta^2}{3}\right)^{1/2}, \qquad (2)$$

$$\eta = (\Phi_{xx} - \Phi_{yy})/\Phi_{zz}; \quad |\Phi_{xx}| \leqq |\Phi_{yy}| \leqq |\Phi_{zz}|.$$

The results are shown in Table 6.

An important finding from Zeeman split NQR is the orientation of the EFGT with respect to the crystal axes. In Table 7 the direction cosines of the

Table 8. Angles between the principal axes of the EFGTs and structure elements (bonds, normal to the ring plane $\boldsymbol{n}$ etc.).

$\sphericalangle(\Phi_{zz}^{(1)}, \mathrm{C}^{(1)}-\mathrm{Cl}^{(1)}) = 1.52°$
$\sphericalangle(\Phi_{zz}^{(1)}, \Phi_{zz}^{(2)}) = 61.53°$
$\sphericalangle(\Phi_{zz}^{(2)}, \mathrm{C}^{(3)}-\mathrm{N}^{(3)}) = 62.98°$
$\sphericalangle(\Phi_{xx}^{(1)}, \boldsymbol{n}) = 2.08°$
$\sphericalangle(\Phi_{yy}^{(1)}, \boldsymbol{n}) = 90.07°$
$\sphericalangle(\Phi_{zz}^{(1)}, \boldsymbol{n}) = 92.02°$
$\sphericalangle(\Phi_{xx}^{(2)}, \boldsymbol{n}) = 5.32°$
$\sphericalangle(\Phi_{yy}^{(2)}, \boldsymbol{n}) = 95.11°$
$\sphericalangle(\Phi_{zz}^{(2)}, \boldsymbol{n}) = 91.22°$
$\sphericalangle(\Phi_{zz}^{(2)}, \mathrm{C}^{(2)}-\mathrm{Cl}^{(2)}) = 1.21°$
$\sphericalangle(\mathrm{C}^{(1)}-\mathrm{Cl}^{(1)}, \mathrm{C}^{(2)}-\mathrm{Cl}^{(2)}) = 60.80°$
$\sphericalangle(\mathrm{C}^{(2)}-\mathrm{Cl}^{(2)}, \mathrm{C}^{(3)}-\mathrm{N}^{(3)}) = 62.20°$
$\sphericalangle(\mathrm{C}^{(1)}-\mathrm{Cl}^{(1)}, \boldsymbol{n}) = 92.17°$
$\sphericalangle(\mathrm{C}^{(2)}-\mathrm{Cl}^{(2)}, \boldsymbol{n}) = 90.97°$

EFGT principal axes and the corresponding bonds ($\mathrm{C}^{(j)}-\mathrm{Cl}^{(j)}$) are given with respect to the orthogonal system X, Y, Z (see Figure 1). The direction cosines are defined in the usual way, e.g. $\lambda^{(j)} = \cos(\Phi_{vv}, X)$, $v = x, y, z$. To aid the discussion, the results given in Table 7 are transferred into angles in Table 8.

Discussion

The crystal structure is shown in a projection along the shortest crystal axis $\boldsymbol{a}$ in Figure 4. The molecules are tilted a little against the plane (100) and a van der Waals packing is observed. The length of the short axis $\boldsymbol{a}$ is 381 pm, corresponding to the van der Waals thickness of a dichloronitrobenzene molecule. In Fig. 5 the intramolecular distances and angles are shown. It is seen that the C–C distances are not equal within the benzene ring. There is a small stretching of the bonds $\mathrm{C}^{(1)}-\mathrm{C}^{(2)}$ and $\mathrm{C}^{(2)}-\mathrm{C}^{(3)}$, which is reflected by a contraction of the angle $\sphericalangle(\mathrm{C}^{(1)}-\mathrm{C}^{(2)}-\mathrm{C}^{(3)})$ from 120° to 117° and a widening of the angle $\sphericalangle(\mathrm{C}^{(2)}-\mathrm{C}^{(3)}-\mathrm{C}^{(4)})$ from 120° to 122.5°. One can also observe a weak tendency of the benzene ring to deform to a boat form; $\mathrm{C}^{(1)}$ and $\mathrm{C}^{(4)}$ are slightly below the average plane of the ring. $\mathrm{Cl}^{(1)}$ follows this deviation, being 8 pm below the plane, whereas the out-of-plane position of $\mathrm{Cl}^{(2)}$ is less pronounced and $\mathrm{N}^{(3)}$ is again in plane. The $\mathrm{NO_2}$ group is rotated around the $\mathrm{C}^{(3)}-\mathrm{N}^{(3)}$ bond, $\mathrm{O}^{(3,1)}$ and $\mathrm{O}^{(3,2)}$ being below and above the ring plane, respectively. The twist angle of the $\mathrm{NO_2}$ group against the ring plane is 53.4°.

The ^{35}Cl NQR measurements show the following features: The temperature dependence of the ^{35}Cl NQR frequencies of $\mathrm{Cl}^{(1)}$ and $\mathrm{Cl}^{(2)}$ is "normal" (see Fig. 2 and Table 5). Without knowledge of IR-Raman spectroscopic data, the change of the density with temperature, and the variation of the molecular geometry as a function of temperature a detailed discussion of $\nu(^{35}\mathrm{Cl}) = f(T)$ within the frame work of the Bayer theory is probably not worthwhile.

As observed for all ^{35}Cl EFGTs of Cl atoms bound to carbon atoms, the direction of $\Phi_{zz}^{(j)}$ is dominated by the bond direction $\mathrm{C}^{(j)}-\mathrm{Cl}^{(j)}$. As reported for $2,6\text{-}\mathrm{Cl_2C_6H_3NHCOCH_3}$ [3], $2,3,6\text{-}\mathrm{Cl_3C_6H_2OCOCH_3}$ [1], and $1\text{-Cl-}3\text{-}\mathrm{NO_2C_6H_4}$ [2], there is a difference between the angle ($\mathrm{C}^{(j)}-\mathrm{X}^{(j)}$, $\mathrm{C}^{(j+1)}-\mathrm{X}^{(j+1)}$) observed by X-ray diffraction and the angle ($\Phi_{zz}^{(j)}$, $\mathrm{C}^{(j+1)}-\mathrm{X}^{(j+1)}$) and the angle ($\Phi_{zz}^{(j)}$, $\Phi_{zz}^{(j+1)}$) observed by single crystal NQR. The effect is also seen but is less pronounced while comparing the angle ($\mathrm{C}^{(j)}-\mathrm{X}^{(j)}$, $\mathrm{C}^{(j+1)}-\mathrm{X}^{(j+1)}$) (X-rays) with $\sphericalangle(\Phi_{zz}^{(j)}, \mathrm{C}^{(j+1)}-\mathrm{X}^{(j+1)})$. We explain

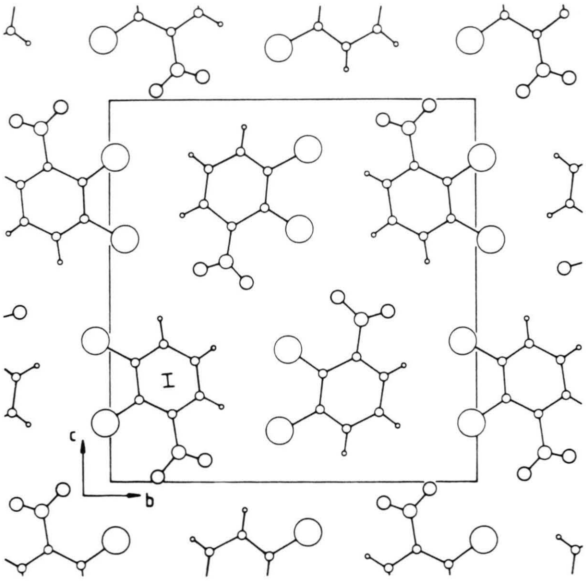

Fig. 4. Projection of the crystal structure of 1,2-dichloro-3-nitrobenzene along [100]. The molecule numbered by I is the one for which the coordinates are given in Table 2.

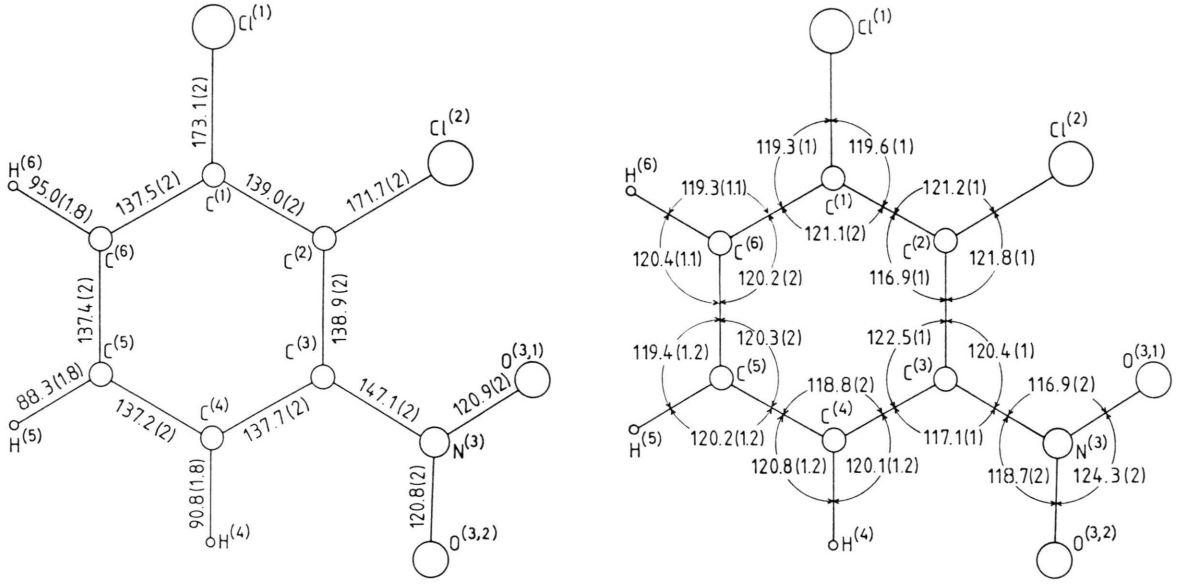

Fig. 5. Molecular geometry parameters of $Cl^{(1)}Cl^{(2)}(NO_2)^{(3)}\,C_6H_3$. *Left:* Intramolecular bond distances. *Right:* Intramolecular bond angles.

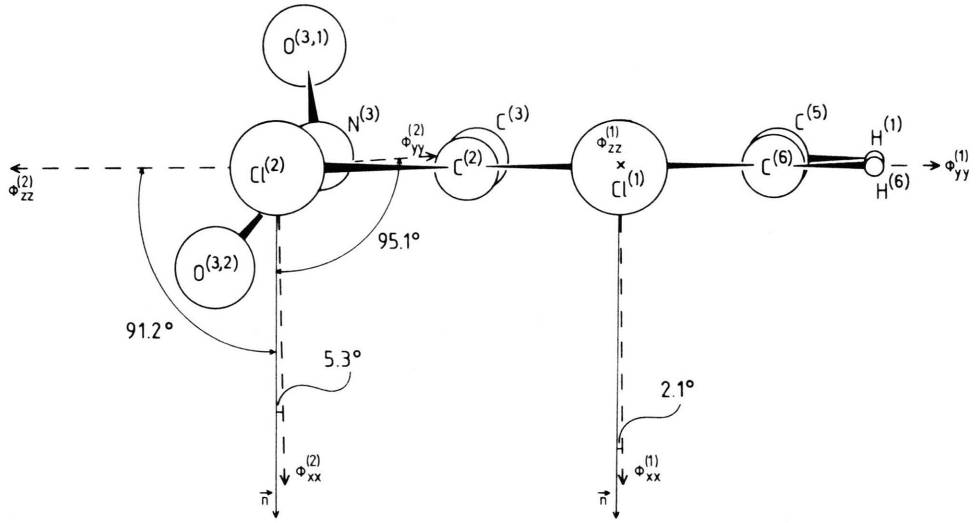

Fig. 6. Projection of the molecule 1,2-Cl_2-3-$NO_2C_6H_3$ along the axis $\Phi_{zz}(Cl^{(1)})$. The angles of the axes $\Phi_{vv}(Cl^{(1)})$, $v = x, y, z$, with respect to the normal $\boldsymbol{n}$ of the "best" plane through $C^{(1)} \ldots C^{(6)}$ are given.

this observation by assuming a repulsion of the electron clouds of $X^{(j)}$ and $X^{(j+1)}$, which affects the outer shell electrons more strongly than the closed shell electrons. While X-ray diffraction weighs all electrons equally, NQR almost neglects the core electrons. To a first approximation a widening of the angles observed by ^{35}Cl NQR with respect to the diffraction results is expected. From Table 8 it is seen that $\sphericalangle(\Phi_{zz}^{(1)}, \Phi_{zz}^{(2)})$ is 0.7° larger than the corresponding bond angle ($C^{(1)}-Cl^{(1)}$, $C^{(2)}-Cl^{(2)}$). Similarly the angle ($\Phi_{zz}^{(2)}$, $C^{(3)}-N^{(3)}$) is 0.7° larger than the corresponding angle ($C^{(2)}-Cl^{(2)}$, $C^{(3)}-N^{(3)}$).

In the discussion and in the figures we handle the principal axes Φ_{xx}, Φ_{yy}, Φ_{zz} as if they were vectors

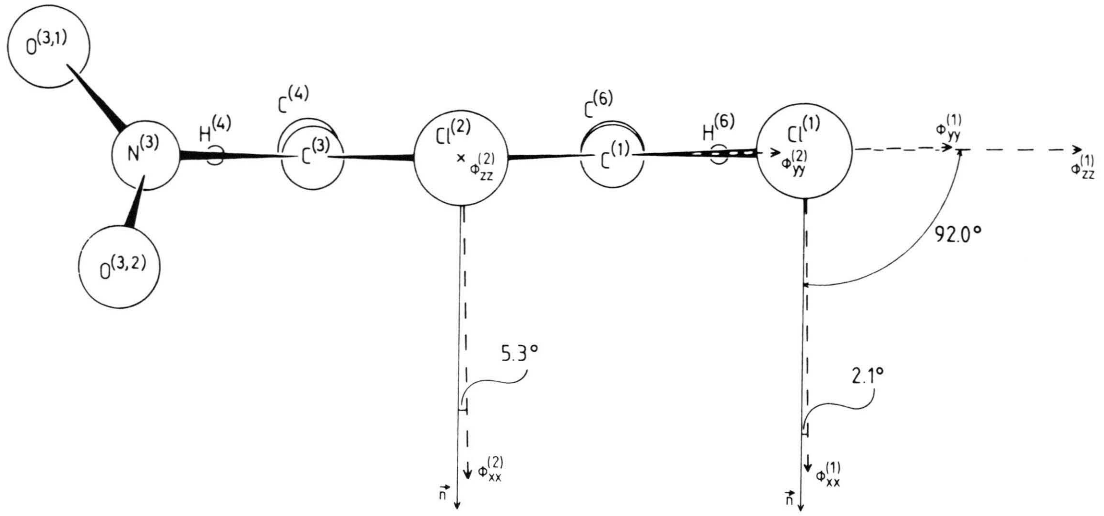

Fig. 7. Projection of the molecule 1,2-Cl_2-3-$NO_2C_6H_3$ along the axis $\Phi_{zz}(Cl^{(2)})$. The angles of the axes $\Phi_{vv}(Cl^{(2)})$, $v = x, y, z$, with respect to the normal $\boldsymbol{n}$ of the "best" plane through $C^{(1)} \ldots C^{(6)}$ are given.

even though they have second rank tensor properties. This is done to avoid the ± signs and to correlate them directly to the direction cosines given in Table 7, where the signs are chosen in such a way that $\Phi_{zz} \parallel$ C−Cl, etc.

In Fig. 6 the molecule $Cl^{(1)}Cl^{(2)}(NO_2)^{(3)}C_6H_3$ is projected along the $C^{(1)}-\Phi_{zz}^{(1)}$ axis. It is seen that $\Phi_{xx}^{(1)}$ is perpendicular to the ring plane, deviating a little (2.08°) from the normal $\boldsymbol{n}$ of the best plane through the ring. $\Phi_{xx}^{(2)}$ is tilted slightly more; the angle $\sphericalangle(\boldsymbol{n}, \Phi_{xx}^{(2)})$ is 5.32°. $\Phi_{yy}^{(1)}$ is almost in the plane of the benzene ring at an angle 90.07° with the normal $\boldsymbol{n}$, as shown in Figure 7. Similarly $\Phi_{yy}^{(2)}$ is also deviating a little from the benzene plane; the angle $(\boldsymbol{n}, \Phi_{yy}^{(2)})$ is 95.11°. In comparison to $\Phi_{xx}^{(1)}$, $\Phi_{yy}^{(1)}$, the more pronounced rotation of the axes $\Phi_{xx}^{(2)}$, $\Phi_{yy}^{(2)}$ with respect to the normal $\boldsymbol{n}$ is due to the polarizing action of the oxygens $O^{(3,1)}$ and $O^{(3,2)}$. We observe that the larger nuclear quadrupole coupling constant of $Cl^{(2)}$ compared to that of $Cl^{(1)}$ is accompanied by a larger increase of $\eta(^{35}Cl)$ from 0.129 to 0.153.

The η-values of $Cl^{(1)}$ and $Cl^{(2)}$ are in the range usually found for aromatic systems. The fact that $\eta(Cl^{(2)})$ is considerably larger than $\eta(Cl^{(1)})$ may be due to two reasons:

(i) $Cl^{(2)}$ is located between two polarizing neighbours, $Cl^{(1)}$ and the NO_2 group, which may lead to a larger deformation of the charge distribution than for $Cl^{(1)}$, which has only one such neighbour.

(ii) $Cl^{(2)}$ is in ortho position to NO_2 and to $Cl^{(1)}$, leading to a higher NQR frequency, in agreement with the Hammett σ-values. From the ^{35}Cl data of aromatic systems obtained by Zeeman split NQR it is found that the σ-relation holds for $e^2\Phi_{zz}Qh^{-1}(^{35}Cl)$. It seems that some kind of such a relation exists for η values, too. Of course more reliable experimental data for a number of compounds must be obtained to prove this assumption.

Acknowledgements

We are grateful to the Deutsche Forschungsgemeinschaft and to the Fonds der Chemischen Industrie for support of this work.

[1] N. Weiden, H. Paulus, and Al. Weiss, J. Mol. Struct. **111,** 301 (1983).
[2] S. Sharma, H. Paulus, N. Weiden, and Al. Weiss, Z. Kristallogr. **171,** 101 (1985).
[3] V. Nagarajan, H. Paulus, N. Weiden, and Al. Weiss, to be published.
[4] F. M. Jaeger, Z. Kristallogr. **42,** 166 (1977).
[5] P. Groth, Chemische Kristallographie **4,** 22 (1917).
[6] V. Nagarajan, N. Weiden, R. Wendel, and Al. Weiss, J. Magn. Reson. **47,** 28 (1982).
[7] V. Nagarajan, Curr. Sci **31,** 233 (1962).
[8] D. Sasikala and C. R. K. Murty, J. Phys. Soc. Japan **23,** 139 (1967).
[9] M. S. Vijava and J. Ramakrishna, J. Chem. Phys. **53,** 4724 (1970).